

MICROSTRIP BANDPASS FILTER USING TRIANGULAR PATCH RESONATOR
FOR WiMAX APPLICATIONS

MOHD RIDZUAN BIN ABDUL RAHMAN

A project report submitted in partial
fulfillment of the requirement for the award of the
Degree of Master of Electrical Engineering

Faculty of Electrical & Electronic Engineering
Universiti Tun Hussein Onn Malaysia

MARCH 2013

ABSTRACT

Filters are essential in *communication* systems nowadays. They are usually used to select frequencies. Filters are playing an important role to select or confine the Radio Frequency (RF) signals within assigned spectral limits since the electromagnetic spectrum is limited by licensing issues and shared over different channels. A compact bandpass filter (BPF) using Triangular Patch Resonator is designed. A 5.5GHz dual-mode microstrip BPF has been introduced. In order to simulate the BPF performance with different configurations, a series of simulations based on Sonnet Lite will be used to run the simulation. Result has been analyzed in terms of reflection coefficient and transmission coefficient. The simulated filter performances are presented.



PT TAA UTAM
PERPUSTAKAAN TUNKU TUN AMINAH

ABSTRAK

Penapis sangat penting digunakan di dalam system komunikasi pada masa kini. Kebiasaannya, penapis digunakan untuk memilih frekuensi tertentu. Penapis juga digunakan untuk memilih atau memasukkan isyarat frekuensi radio di dalam had spectral yang disetkan di mana medan electromagnet adalah terhad disebabkan masalah perlesenan dan perkongsian dengan saluran yang berbeza. Sebuah penapis jalur lulus yang kecil menggunakan Penggetar Berbentuk Segitiga telah diciptakan. Sebuah penapis jalur lulus mikrojalur dua mod yang beroperasi pada $5.5GHz$ telah direkabentuk. Bagi menjalankan simulasi pencapaian penapis jalur lulus dengan kaedah yang berbeza, sebuah simulasi berasaskan Sonnet Lite telah digunakan untuk melaksanakan simulasi ini. Hasil simulasi telah dianalisis berdasarkan kecekapan pantulan dan kecekapan penghantaran. Hasil simulasi bagi pencapaian penapis telah di perseMBahkan.



PERPUSTAKAAN TINGKATAN AMINAH

CONTENTS

TITLE	i
DECLARATION	ii
DEDICATION	iii
ACKNOWLEDGEMENTS	iv
ABSTRACT	v
ABSTRAK	vi
CONTENTS	vii
LIST OF TABLES	ix
LIST OF FIGURES	x
LIST OF SYMBOLS / ABBREVIATIONS	xiii
CHAPTER 1 INTRODUCTION	1
1.1 Background	1
1.2 Aims and objectives	3
1.3 Project motivation	3
CHAPTER 2 LITERATURE REVIEW	4
2.1 Microstrip filter	4
2.1.1 Microstrip Lines	5
2.1.1.1 Dielectric Constant	6
2.1.1.2 Effective Dielectric Constant	6
2.1.1.3 Characteristic Impedance	8
2.1.2 Microstrip Resonators	10
2.1.2.1 Triangular Patch Resonators	10

2.1.2.2 Bandwidth	15
CHAPTER 3 METHODOLOGY	16
3.1 Introduction	16
3.2 Sonnet Lite Software	17
CHAPTER 4 DATA ANALYSIS AND RESULT	27
4.1 Introduction	27
4.2 Analysis for gap variation between two transmission lines	27
4.3 Analysis for gap variation between triangular resonator and transmission lines	33
4.4 Analysis for variation length of triangular resonator	37
4.5 Analysis for two triangular patch resonators with varies the size of bottom triangular	43
4.6 Analysis for two triangular patch resonator with varies the size of top triangular	47
CHAPTER 5 CONCLUSION AND RECOMMENDATION	52
5.1 Conclusion	52
5.2 Recommendation	53
REFERENCES	54



LIST OF TABLES

4.1	Result analysis for different gaps between two transmission lines for Gap $0.2mm$, $0.6mm$ and $1mm$.	30
4.2	Result analysis for different gaps between two transmission lines for Gap $1mm$, $1.4mm$ and $1.8mm$	31
4.3	Result analysis for different gaps between two transmission lines for Gap $1mm$, $5mm$ and $9mm$.	31
4.4	Result analysis for different gaps between triangular and transmission line for Gap $0.2mm$, $0.4mm$ and $0.6mm$.	34
4.5	Result analysis for different gaps between triangular and transmission line for Gap $0.1mm$, $0.2mm$ and $0.3mm$.	36
4.6	Result analysis for different lengths of the triangular for Length Triangular $9mm$, $11mm$ and $13mm$.	39
4.7	Result analysis for different lengths of the triangular for Length Triangular $11mm$, $15mm$ and $19mm$	41
4.8	Result analysis for different length at the bottom triangular for Bottom Triangular Length $12mm$, $13.4mm$ and $14.1mm$	45
4.9	Result analysis for different length at the bottom triangular for Bottom Triangular Length $10mm$, $11.2mm$ and $12mm$	47
4.10	Result analysis for different length at the top triangular for Top Triangular Length $12.6mm$, $13.4mm$ and $14.3mm$	49

LIST OF FIGURES

2.1	Microstrip substrate	5
2.2	Equivalent geometry of quasi-TEM microstrip line	7
2.3	Result simulated with different effective dielectric constant	8
2.4	Current distributions of the first two modes of a triangular microstrip resonator	10
2.5	Stimulated resonant frequencies of the first two modes of triangular microstrip resonator.	11
2.6	Fabricated filter using triangular microstrip resonators operating at the mode 2	12
2.7	Fabricated filter using triangular microstrip resonators operating at the mode 2 filter designed	13
3.1	Sonnet Software Logo	16
3.2	Sonnet Task Bar	17
3.3	New Geometry in the project Sonnet task bar	18
3.4	Sonnet Project Editor	19
3.5	Unit dialog box	20
3.6	Box setting dialog box	20
3.7	Estimated memory dialog box	21
3.8	Dielectric layer dialog box	21
3.9	Metal type dialog box	22
3.10	Sonnet project editor dialog box	23
3.11	Analysis setup dialog box	24
3.12	Sonnet analysis monitor dialog box	25
3.13	Result frequency response	26

4.1	Layout of a dual mode microstrip triangular patch resonator	28
4.2	Simulated frequency response for gap, $g=1\text{mm}$	28
4.3	Simulated frequency response for gap, $g=0.2\text{mm}$, 0.6mm and 1mm .	29
4.4	Simulated frequency response for gap, $g=1.0\text{mm}$, 1.4mm and 1.8mm	30
4.5	Simulated frequency response for gap, $g=1\text{mm}$, 5mm and 9mm	31
4.6	Simulated frequency response for gap, $b=0.2\text{mm}$, 0.4mm and 0.6mm	33
4.7	Simulated frequency response for gap, $b=0.1\text{mm}$, 0.2mm and 0.3mm .	35
4.8	Simulated frequency response for gap 1mm between triangular and transmission line	36
4.9	Simulated frequency response for gap 2mm between triangular and transmission line	37
4.10	Simulated frequency response for length, $a=9\text{mm}$, 11mm and 13mm .	38
4.11	Simulated frequency response for length, $a=11\text{mm}$, 15mm and 19mm	40
4.12	Layout of dual mode triangular patch resonator	41
4.13	Simulated S-parameter for dual mode triangular resonator	42
4.14	Layout of a dual mode microstrip triangular patch resonator	43
4.15	Simulated frequency response for bottom triangular size, $y=12\text{mm}$, 13.4mm and 14.1mm	44
4.16	Simulated frequency response for bottom triangular size, $y=10\text{mm}$, 11.2mm and 12mm .	46
4.17	Simulated frequency response for top triangular size, $y=12.6\text{mm}$, 13.4mm and 14.3mm .	48



4.18	Layout design for dual mode triangular patch resonator	50
4.19	Simulated S-parameter dual mode triangular patch resonator	51



PTTHM
PERPUSTAKAAN TUNKU TUN AMINAH

LIST OF SYMBOLS AND ABBREVIATIONS

D, d	Diameter
$G Hz$	Giga Hertz
h	Thickness of substrate
L	Length of microstrip
mm	Milimeter
t	Thickness of conductor
W	Width of microstrip
ϵ_{eff}	Effective permittivity
ϵ_o	Relative permittivity of free space
ϵ_r	Relative permittivity of substrate
μ_o	Permeability constant
λ_g	Guided wavelength
λ_o	Free space wavelength
f_1	Lower cutoff frequency
f_2	Upper cutoff frequency
f_c	Center frequency
g	Prototype element value
S_{11}	Reflection coefficient
S_{21}	Transmission coefficient
TEM	Transverse electromagnetic
ω	Angular frequency in radian/s ⁻¹
Z_o	Input Impedance
Φ	Phase angle or electrical length
Ω	Ohms

<i>EM</i>	Electromagnetic
<i>FFT</i>	Fast Fourier Transform
<i>MB</i>	Mega Byte
<i>BPS</i>	Bandpass Filter
<i>dB</i>	Decibel
<i>MEMS</i>	Micro Electromagnetic
<i>HTS</i>	High Temperature Superconductor
<i>LTCC</i>	Low temperature co fired ceramics
<i>MMIC</i>	Monolithic microwave integrated circuits
<i>WiMax</i>	Worldwide Interoperability for Microwave Access



PTTA UTHM
PERPUSTAKAAN TUNKU TUN AMINAH

CHAPTER 1

INTRODUCTION

1.1 Background

Bandpass filter is designs that allow signal to pass through a desired frequency range and rejects other unwanted frequencies outside the desired range. The new technology for mobile and wireless *communication* system has increased the need of applying the microstrip bandpass filters into design. Also the resonators are usually used in design of antennas [1], filters [2], [3], microwave circuits and systems due to microstrip patch resonators have many attractive features.

In general, microstrip bandpass filters can be designed either single- or dual-mode resonators. The basic principle for designing a patch resonator filter is the selectivity and application of all sorts of resonant modes. Currently, microwave patch filters design dominantly concentrates on dual-mode (the dominant mode and its degenerate mode) operation; however, the higher order modes are not applied. Dual-mode microstrip resonators are interesting because each of the dual-mode resonators can be used as a doubly tuned resonant circuit. Besides that, the nuMber of resonators required for a given degree filter is reduced by half, resulting in a compact filter configuration [4]–[8].

Several types of dual-mode microstrip resonators have been used, including the circular ring [5], meander loop [6], circular disk, square patch [7], [8] and triangular patch resonator. Triangular patch filters behave good performances in RF and modem communication systems. However, limited works are reported compared with the square and circular patch filters. Although microstrip filters using triangular patch resonators have been reported recently [9], each of the triangular patches operates merely with a single mode at a certain frequency band. The triangular patch is an interesting element. However, up to date, only single-mode operations have been reported [9]–[11], [12].

Patch resonator filters are popular for the advantages of lower cost, easier fabrication, more compact and smaller structures, lower loss and higher power handling features compared with the line-based resonator filters. Low insertion loss, high return loss and high rejection band are the desired characteristics of a good filter. The advanced filtering characteristics with transmission zeros have been demanded to improve the selectivity, sensitivity and efficiency of spectrum utilization. However, there was no transmission zero on the high stopband in [4]. There was only one transmission zero in [4]. This work stemmed from the above mention concerns.

In this project, dual mode bandpass filter using triangular resonator at frequency $5.5GHz$ are designed for the WiMax application. Two transmission zeros can be implemented on the both sides of the passband. The center frequency of filter can be modified by changing the size of triangular notch in the patches. The effects of triangular patches shape and gap size between resonators and two transmission lines have been studied. These new types of bandpass filters have been verified by simulation. Simulated exhibit good performance.

In this project, dual mode bandpass filter using triangular resonator at frequency $5.5GHz$ are designed and simulated using software SONNET LITEPlus. Software Matlab are used to verified the results.

1.2 Aims and objectives

The objective of this project is to design and analyze dual band bandpass filter at 5.5GHz using triangular patch resonator. SONNET Lite simulation software is used to design, simulate and analyze a dual band Bandpass Filter at 5.5GHz using triangular patch resonator. Apart from theoretical knowledge, there will also be involved in a hands-on operation to construct the microstrip filters through effective research methodology to produce excellent design. Furthermore, the project will be able to measure the frequency responses of these prototypes by using the SONNET Lite simulation software and compare the measured result using Matlab software. So, it is important to understand the fundamental knowledge in microstrip filter.

The project aims to design a microstrip bandpass filter which is simple and easy. The design filter must be a dual mode bandpass device that resonates in the frequency range of 5GHz to 6GHz . Otherwise, this project aims to design a dual-mode microstrip triangular resonators and filters at 5.5GHz where the filter will be unique, simple, and high-performing. Through this project, we will have a better understanding of the microstrip bandpass filter properties.

1.3 Project motivation

The project motivation is to design the microstrip bandpass filters that are to fulfill the master's project requirement. After completing the literature review throughout the journals, knowledge in filter design has improved. The aim of this project is to design a simple, high performing, and small size microstrip bandpass filter that has results comparable to those published.

CHAPTER 2

LITERATURE REVIEW

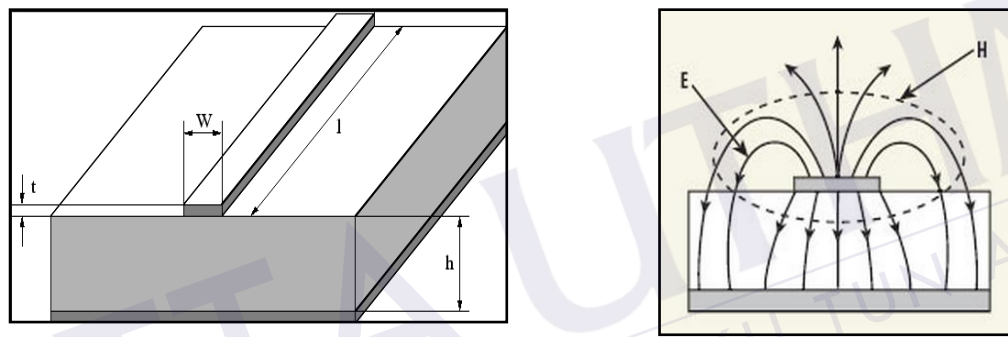
2.1 Microstrip filter

Radio Frequency (RF) and microwave filter are important and essential components for the new modern wireless and mobile communication systems. Otherwise filters are used in the RF and microwave applications due to design for the filters are smaller size, lighter weight, higher performance, and lower insertion loss is of high demand. All the requirements stated above can cover by microstrip filters. There are some application for the microstrip filter such as low-temperature co fired ceramics (*LTCC*), high temperature superconductor (*HTS*), monolithic microwave integrated circuits (*MMIC*), micro electromechanic system (*MEMS*) and micromachining technology, have driven the rapid development of the new microstrip filter than other microwave and RF filters.

Many different requirements for the different pattern can be designed using microstrip filters but for the different design of microstrip filter consists of different individual properties and characteristics. There are some designs for microstrip that available in market is such as rectangular patch filter, circular patch filter, triangular patch filter and etc.

2.1.1 Microstrip Lines

The microstrip line consists of conductor of width W printed on a thin-film strip, grounded dielectric substrate of thickness d and relative permittivity ϵ_r . In a microstrip transmission line the dielectric does not completely surround the conducting strip and consequently the fundamental mode of propagation is not a pure TEM mode. As it can be seen from the Fig. 2.1, most of the field lines are contained in the dielectric region, and some fraction in the air region above the substrate.



(a) Microstrip Line

(b) Electric and magnetic field distribution in the microstrip line

Fig 2.1: Microstrip substrate.

It is similar to stripline and coplanar waveguide, and it is possible to integrate all three on the same substrate. In December 1952 Grieg and Engelmann was developed microstrip by ITT laboratories as a competitor to stripline. According to Pozar, the early microstrip work used fat substrates, which allowed non-TEM waves to propagate which makes results unpredictable. The thin version of microstrip started became famous in 1960s. Printed circuit board (PCB) technology is used to fabricate the microstrip and to convey microwave frequency signals. It consist of a conducting strip separate from a ground plane by a dielectric layer which known as substrate.

Many application of the microstrip likes design antennas, couplers, filters, power dividers and etc. The entire microstrip is just a patterned metal and a ground plane only, so the material costs are lower, much lighter and more compact compare to traditional

waveguides. While the microstrip is not enclosed as a waveguide, it is effect to crosstalk and unintentional radiation. But for the stripline, microstrip can mount all the active components on top of the board. Lower power handling capacity and higher losses are the disadvantages of the microstrip. Other disadvantages are that when high isolation is required such as in a filter or switch, some external shielding may have to be considered. In this project, microstrip has been chosen for the filter design because it is a proven technology and the shielding problem can be solved easily by encapsulating the filter in a metallic box. Besides, crosstalk and unintentional radiation are not an issue in this project as well.

2.1.1.1 Dielectric Constant

Microstrip can be fabricated on different substrates based on the requirement of the design. For a lower cost, microstrip devices can be built on the ordinary Duroid 6006 substrate. Dielectric constant is a measure of the extent to which it concentrates electrostatic lines of flux. For example, *FR-4* has a dielectric constant of 4.4 and R6006 duroid has 6.15 at frequency of 10 GHz. And by definition, the dielectric constant of vacuum is equal to 1. Dielectric constant is frequency dependent.

2.1.1.2 Effective Dielectric Constant

In general, the effective dielectric constant can be interpreted as the dielectric constant of a homogenous medium that replaces the air and dielectric regions of the microstrip (Figure 2.2). This accounts for the fact that the fields around the microstrip line are partly in air (lossless) and partly in dielectric.

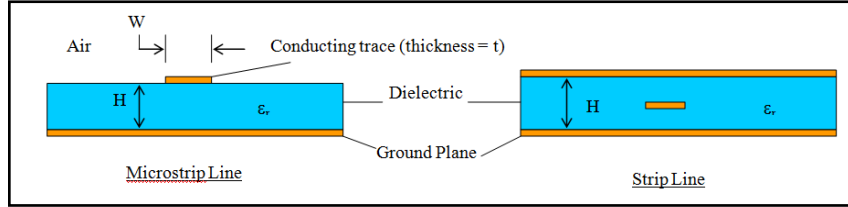


Figure 2.2: Equivalent geometry of quasi-TEM microstrip line [1]

The effective dielectric constant of a microstrip line is approximately given by Pozar [1].

$$\epsilon_{eff} = \frac{\epsilon_r + 1}{2} + \frac{\epsilon_r - 1}{2} \cdot \frac{1}{\sqrt{1 + \frac{12H}{W}}} \quad (2.1)$$

A few other formulas are given by T Edwards [2] and by Hammerstad and Jensen which are reproduced here as follows

$$\epsilon_{eff} = \frac{(\epsilon_r + 1)}{2} + \frac{(\epsilon_r - 1)}{2} (1 + 10/v)^{-ab} \quad (2.2)$$

Where $v = W/d$ and

$$a = 1 + \frac{1}{49} \ln \left(\frac{v^4 + (v/52)^2}{v^4 + 0.432} \right) + \frac{1}{18.7} \ln \left(1 + \left(\frac{v}{18.1} \right)^3 \right) \quad (2.3)$$

$$b = 0.564 \left(\frac{\epsilon_r - 0.9}{\epsilon_r + 3} \right)^{0.053} \quad (2.4)$$

In consequence, the propagation velocity is somewhere between the speed of radio waves in the substrate, and the speed of radio waves in air. This behaviour is commonly described by stating the effective dielectric constant of the microstrip. Effective dielectric constant is an equivalent dielectric constant of an equivalent

homogeneous medium. As part of the fields from the microstrip conductor exists in air, the effective dielectric constant is less than the substrate's dielectric constant.

The formulas given by Edwards, Hammerstad were simulated using MathCAD and compared to simulation done by the program Sonnet. This is shown in Figure 2.3.

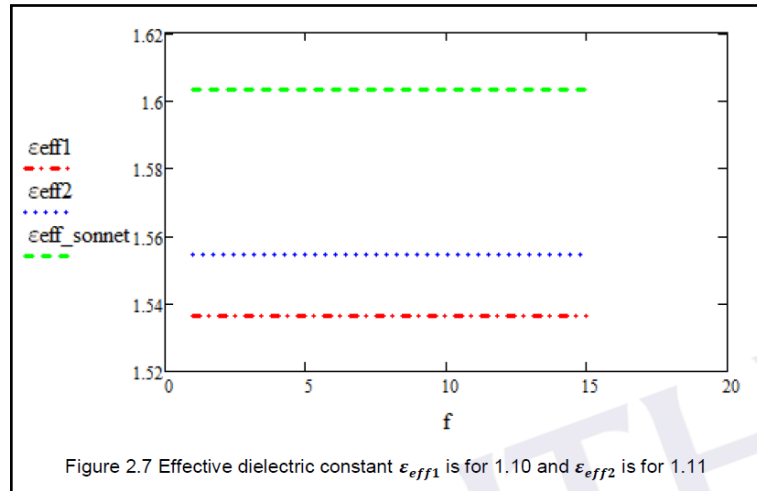


Figure 2.3: Result simulated with different effective dielectric constant

For the Sonnet simulation, a 50Ω line was chosen and $\epsilon_r = 1.96$ was selected for all the simulations. The Sonnet results are at $1GHz$ and the other results are static-*TEM* approximations.

2.1.1.3 Characteristic Impedance

The characteristic impedance, Z_o is important in microstrip lines design, it will affects the reflection loss, S_{11} . The reflection loss is related to the characteristic impedance and also loads impedance by formula,

$$S_{11} = \frac{Z_{in} - Z_o}{Z_{in} + Z_o} \quad (2.5)$$

The characteristic impedance of microstrip must be equal to the input of the impedance to minimize the reflection loss at the input port. Most of the input ports are designed at 50 ohm to prevent any reflections. The characteristic impedance Z_0 is also a function of the ratio of the height to the width W/H (and ratio of width to height H/W) of the transmission line, and also has separate solutions depending on the value of W/H . Note that effective dielectric constant value is required for the microstrip characteristic impedance calculation. The characteristic impedance of microstrip lines can be calculated by using formulas below.

When $\left(\frac{W}{H}\right) \leq 1$

$$Z_o = \frac{60}{\sqrt{\epsilon_{eff}}} \ln\left(8 \frac{H}{W} + 0.25 \frac{W}{H}\right) \text{ohms} \quad (2.6)$$

When $\left(\frac{W}{H}\right) \geq 1$

$$Z_o = \frac{120\pi}{\sqrt{\epsilon_{eff}} \times \left[\frac{W}{H} + 1.393 + \frac{2}{3} \ln\left(\frac{W}{H} + 1.444\right) \right]} \text{ohms} \quad (2.7)$$

The first step in this project is to design the microstrip lines that can achieve 50 ohm of characteristic impedance, Z_0 . From the formulas above, there are three variables in the calculation which are ϵ_{eff} , Width (W) and Height (H). Since the ϵ_{eff} and height is constant for the substrate, the only variable is the width of the microstrip line.

Since the formula is quite complicated, we have to substitute different W value in order to get 50 ohm characteristic impedance. At first, it has to verify the ratio of W/H and determine which formula to be used. It is time consuming for the calculation on different substrate. Fortunately, some of the web application and software are able to calculate the width of the microstrip lines by entering the desire characteristic impedance, height of the substrate and dielectric constant of the substrate. Then the software will perform the calculation within seconds and shows the value. It has

simplified the microstrip lines design work and most importantly consume less time. For instance, one of the useful software was used for characteristic impedance calculation in this project is microstrip calculator. The software is easy to control and able to get the width value easily by key in height of the substrate, thickness of the strip, and dielectric constant of the substrate. The microstrip width calculation will be cover in Methodology part.

2.1.2 Microstrip Resonators

Microstrip resonators can be designed in various patterns. Microstrip resonators are typically coupled through gaps, apertures, slots, or probes. The common types of resonator are open loop resonator, circular, square and triangular patch resonator. The types of resonators that covered are dual mode microstrip triangular resonator.

2.1.2.1 Triangular Patch Resonators

From the paper of Jia-Sheng Hong and Michael J. Lancaster, “Microstrip Triangular Patch Resonator Filter” has been designed on 0.635mm RT/Duroid substrate with a relative dielectric constant of 10.8 and thickness of 12.7mm . The full-wave *EM* simulator is used to this design. This journal has designed and fabricated two three-pole microstrip triangular resonator bandpass filters.

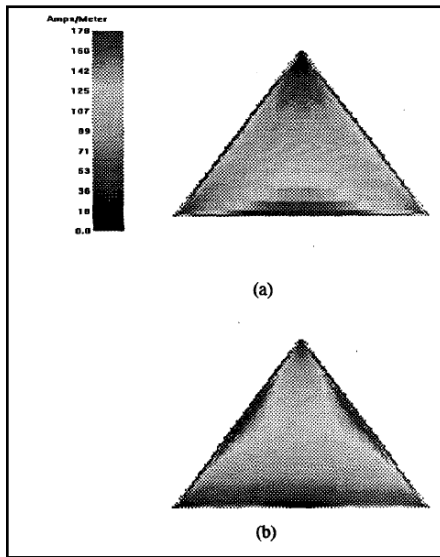


Figure 2.4: Current distributions of the first two modes of a triangular microstrip resonator (a) Mode 1 (b) Mode 2

Fig. 2.4 showed the field distributions of two distinguishable resonant modes of a microstrip triangular patch resonator, which were obtained using a full wave electromagnetic (EM) simulator. It can clearly be identified that the mode 1 in Fig. 2.4(a) has almost current concentrated on the base, whereas the mode 2 in Fig. 2.4(b) has almost current on the both slant sides. It is these two modes that will be operated in filters to result in different filtering characteristics.

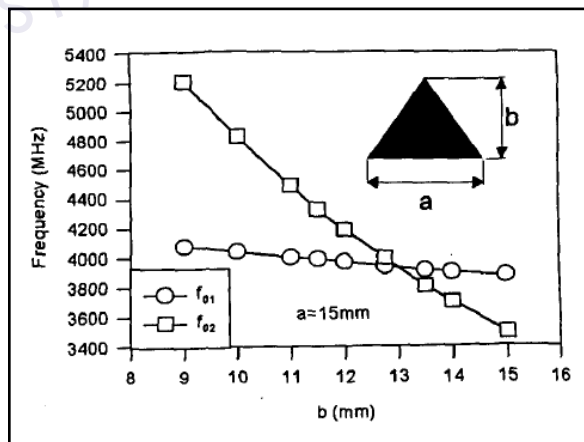
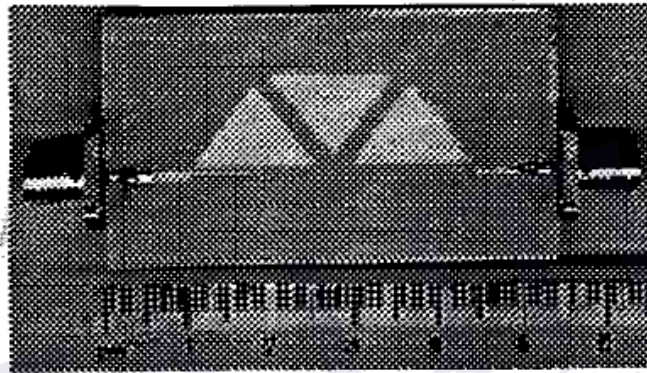
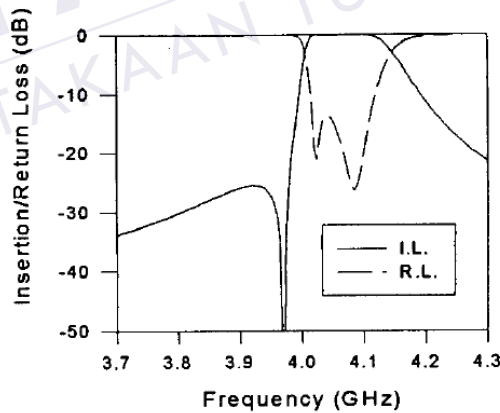


Figure 2.5: Stimulated resonant frequencies of the first two modes of triangular microstrip resonator.

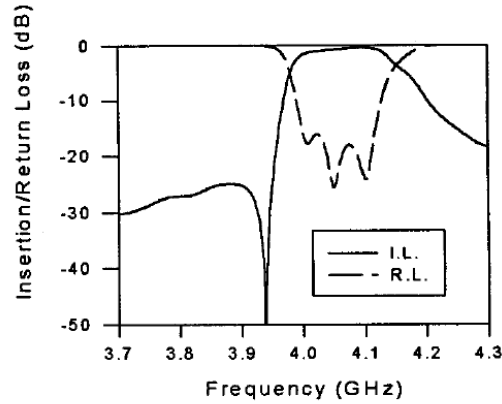
Fig. 2.5 plot some simulated results of the resonant frequencies as a function of the vertical height b for a given base length a . f_{01} is the resonant frequency of mode 1, while f_{02} is the resonant frequency of mode 2. As can be seen f_{01} , the resonant frequency of mode 1 is less dependent on b . This may be understood because this mode is mainly based on the base of the triangle as shown in Fig.2.4 (a). Obviously, one can use this property to control the separation of the two modes. When $b=13mm$ in Fig.2.5, the isosceles triangle degenerates to an equilateral triangle, and the two modes have the same resonant frequencies.



(a)



(b)

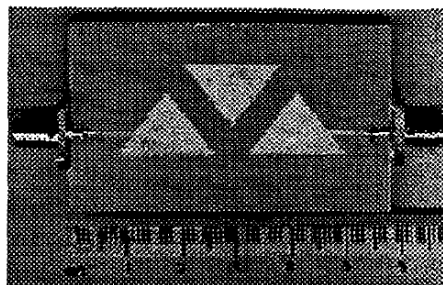


(c)

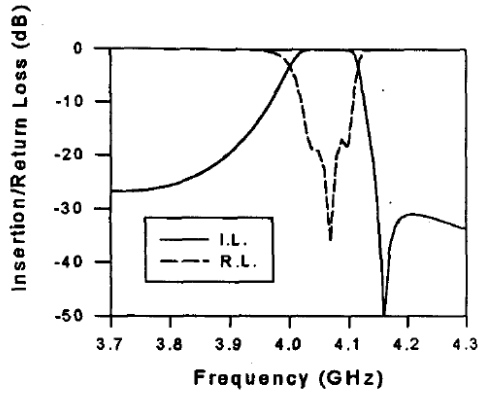
Figure 2.6: (a) Fabricated filter using triangular microstrip resonators operating at the mode 2; (b) Theoretical performance; (c) Experimental performance.

Fig. 2.6(a) shows the fabricated filter that was designed to operate at the resonant mode 1 of Fig. 2.4(a) and to have an asymmetric response with a finite transmission zero on the low stopband. The full-wave EM simulated performance of the filter is plotted in Fig. 2.6(b), while the measured one in Fig. 2.6(c).

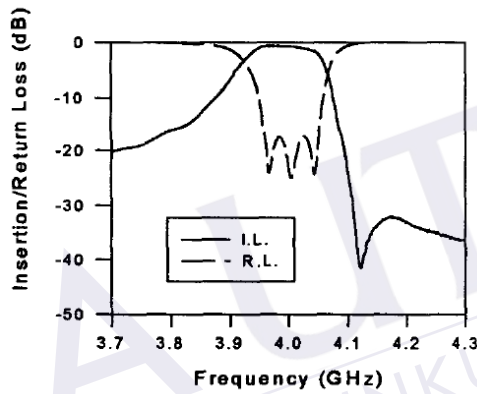
The filter that was designed to operate at the mode 2 of Fig. 2.4(b) and to have a finite frequency transmission zero located on the high stopband is illustrated in Fig. 2.7(a). It should be noticed that despite of a similarity of the cascaded resonator structure with Fig. 2.6(a), the input and output coupling structures and locations in the two filters are different because they operate at different modes. The full-wave EM simulated performance of the filter is plotted in Fig. 2.7(b), while the measured one in Fig.2.7(c), where the finite-transmission zero as compared with the previous filter is located on the other side of the passband, improving the selectivity on that side as what is desired.



(a)



(b)



(c)

Figure 2.7: (a) Fabricated filter using triangular microstrip resonators operating at the mode 2 filter designed; (b) Theoretical performance; (c) Experimental performance.

In this journal, the different approach for triangular patch resonator to have transmission zeros was studied. The author demonstrated that microstrip triangular patch resonator filters could have some advanced filtering characteristics in a simple circuit topology of cascading resonators.

2.1.2.2 Bandwidth

The fundamental definition of the bandwidth of an antenna is the difference between the upper and lower frequencies of operation (f_H and f_L respectively)

$$bw = f_H - f_L \quad (2.8)$$

For all that, the spectrum managers often use a variety of different bandwidth definitions, including fractional or percent bandwidth. These measures of relative bandwidth require the calculation of a central frequency, which is either the arithmetic or geometric average of the upper and lower frequencies. The center frequency is defined as the arithmetic average of the upper and lower frequencies

$$f_C = \frac{f_H + f_L}{2} \quad (2.9)$$

An arithmetic average yields the central frequency when frequency is considered on a linear scale. An alternate definition of center frequency involves the geometric average

$$f_C = \sqrt{f_H f_L} \quad (2.10)$$

The geometric average yields the center frequency when frequency is considered on a logarithmic scale and is less commonly used. So the arithmetic average should be assumed unless otherwise is specified. The fractional bandwidth of a system is the ratio of the bandwidth to the center frequency (either the geometric or the arithmetic definition is used)

$$BW = \frac{bw}{f_C} \quad (2.11)$$

Alternatively, fractional bandwidth may be defined on a percentage basis

$$BW\% = \frac{bw}{f_c} 100\% \quad (2.12)$$

Since the geometric definition of center frequency always yields a frequency smaller than the arithmetic average, fractional bandwidths calculated using the geometric definition are always larger than the arithmetic ones. So, the designer of the filter has to pay attention on which definition is used.



PTTA UTHM
PERPUSTAKAAN TUNKU TUN AMINAH

CHAPTER 3

METHODOLOGY

3.1 Introduction

In providing a general platform for simulation, software which is able to simulate the circuit as well as the layout based design is chosen. This software is called Sonnet Lite as it is shown in Figure 3.1. Sonnet Lite is used to design and simulate frequency response for resonators and filters. This project only focuses on simulation experiment and not covers to fabricate the hardware of the project due to constraint of time and cost of fabricate.



Figure 3.1: Sonnet Software Logo

The *Sonnet EM* analysis is based on a method-of-moments technique. The circuit metal is first meshed into small subsections. The *EM* coupling between each possible pair of subsections is calculated and this fills a big matrix. The matrix is inverted, yielding all currents everywhere in the circuit metal. This, in turn, determines things like S-parameters, which can be used in other analysis programs.

The Sonnet analysis has very high accuracy because it calculates all couplings between subsections using a 2-D Fast Fourier Transform (*FFT*). In signal processing, application of the *FFT* requires uniform time sampling of a signal. In *EM* analysis, the *FFT* requires uniform space sampling across the two dimensions of the substrate surface. Thus the analyzed circuit metal falls on a uniform underlying *FFT* mesh. The *FFT* approach also requires the circuit to exist inside a conducting, shielding box. Approximations are available to include radiation. A common alternative technique requires a four dimensional numerical integration to calculate each pair-wise coupling. This approach has the advantage of eliminating the underlying uniform mesh, however, it comes at the cost of sometimes extensive numerical integration time and the additional error involved in the numerical integration process. The *FFT* used by Sonnet quickly calculates all couplings to full numerical precision. In contrast to the *FFT* approach, numerical integration requires an open environment allowing radiation while a shielded environment must be approximated.

When and if a serious planar numerical integration based *EM* tool becomes freely available, the user will find the relative advantages and disadvantages tend to compliment Sonnet's *FFT* based tool.

3.2 Sonnet Lite Software

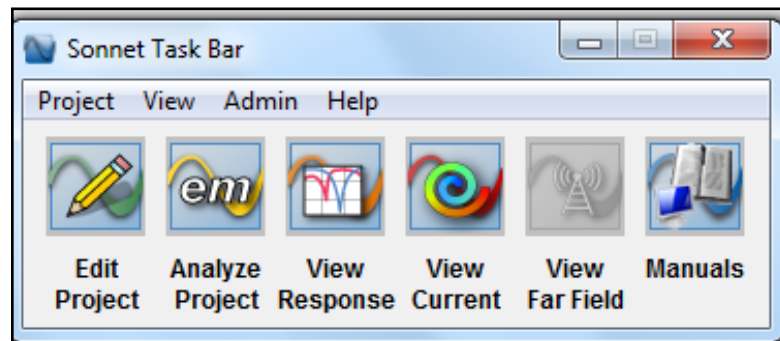


Figure 3.2: Sonnet Task Bar

After open the Sonnet Lite software, the Sonnet task bar appears on computer display. The *Sonnet Task Bar* allows accessing all the modules in Sonnet Software, managing the project files, accessing the online manuals and Sonnet example files and accessing various administrative tasks. There have some icon to be selected. It have edit project, analyze project, view response and view current. The project editor is a user-friendly graphical interface that enables designer to input a circuit geometry or circuit netlist for subsequent *em* analysis. Analysis controls project can be set up in the *project editor*.

Em is the electromagnetic analysis engine. It uses a modified method of moments analysis based on Maxwell's equations to perform a true three dimensional current analysis of predominantly planar structures. *Em* computes S, Y, or Z-parameters, transmission line parameters (Z_o , ϵ_{eff} , $VSWR$, G_{max} , Z_{in} , and the Loss Factor), and SPICE equivalent lumped element networks. Additionally, it creates files for further processing by the current density viewer and the far field viewer. *Em*'s circuit netlist capability cascades the results of electromagnetic analyses with lumped elements, ideal transmission line elements and external S-parameter data.

The response viewer is the plotting tool. This program allows you to plot your response data from *em*, as well as other simulation tools, as a Cartesian graph or a Smith chart. You may also plot the results of an equation. In addition, the response viewer may generate Spice lumped models.

The current density viewer is a visualization tool which acts as a post-processor to *em* providing you with an *immediate* qualitative view of the electromagnetic interactions occurring within your circuit. The currents may also be displayed in 3D.

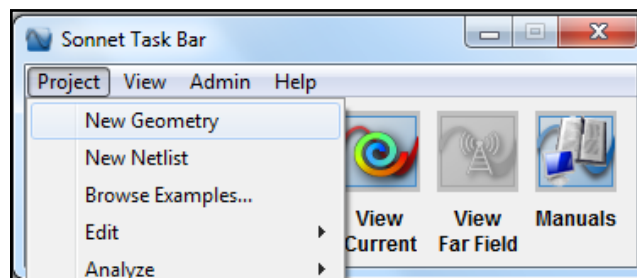


Figure 3.3: New Geometry in the project *Sonnet task bar*

Button Project in the *Sonnet task bar* is click and a pop-up menu appears on the task bar. New Geometry from the pop-up menu is select.

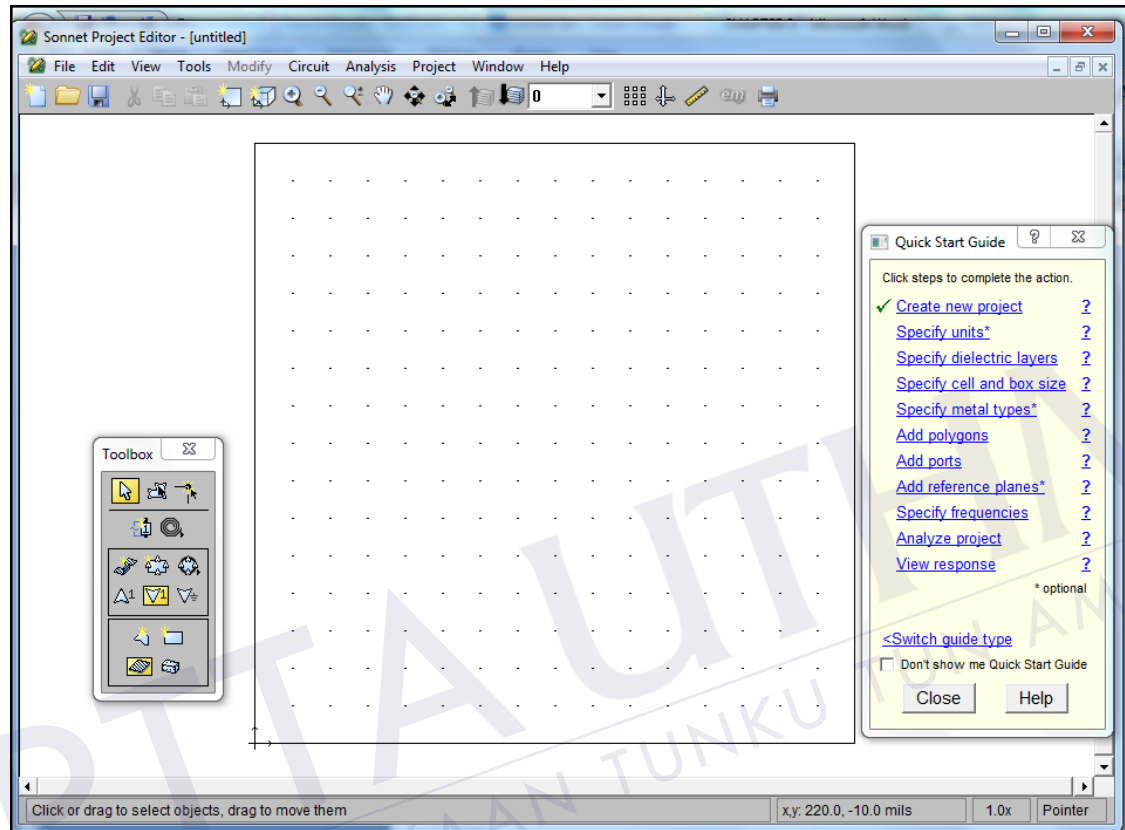


Figure 3.4: Sonnet Project Editor

A project editor window, with an empty substrate, appears on computer display as shown at above. The view shown in the project editor window is a two-dimensional view from the top looking directly down on the substrate. The tool box, which allows easy access to commonly used functions, also appears on your display. The Quick Start Guide also appears on the display. This guide provides step by step directions in how to create circuit geometry in the project editor, including how to import a *GDSII* or *DXF* file. The *Quick Start Guide* keeps track of which steps have been done allowing you to use the guide as a task list as well as an instructor.

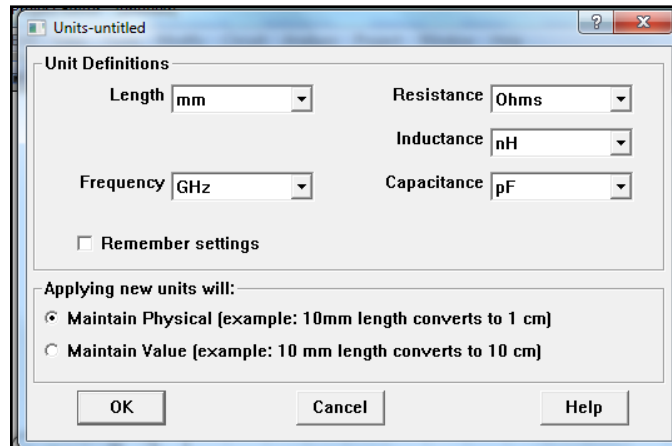


Figure 3.5: Unit dialog box.

This *dialog box* is used to set the unit definitions for length and frequency. The unit is set *mm* for the length and *GHz* for the frequency. To set this unit, click the circuit on the tool bar and select units.

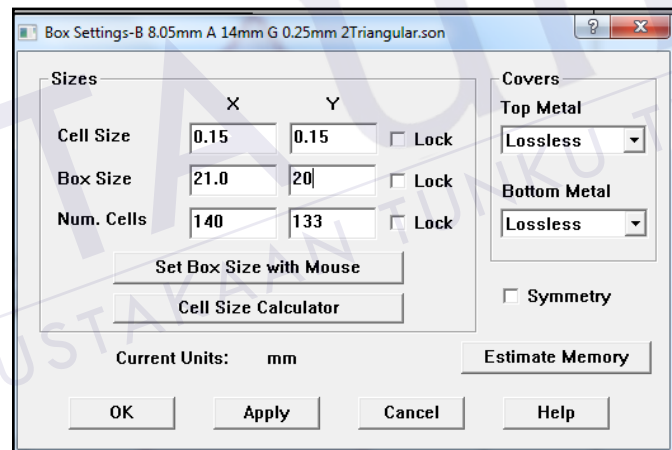


Figure 3.6: Box setting dialog box.

The *Box Settings* dialog box in order to display the parameters of the circuit box, as well as to allow for modification of those parameter values. The default box size for a new circuit is *160 mils X 160 mils* with a cell size of *10 mils X 10 mils*. Cell Size is the size of a single cell of the box area. The X dimension (width) and a Y dimension (height) need to set. Selecting cell size is important. The *EM* analysis automatically subsections the circuit based on the cell size. Small cells result in slower but more accurate analyses. In this project, the cell size is set depend on the design to achieve bigger memory but memory is must be less than *32MB* for the memory size. This project is set *0.15mm* to X

dimension and 0.15mm to *Y* dimension. *Box Size* is the size of the box area. The *X* dimension (width) and a *Y* dimension (height) need to set. In this project, box size is set to 21mm to *X* dimension and 20mm to *Y* dimension. *Num. Cells* is the nuMBER of cells in the box area. *Num. Cells* automatically depends on value of the cell size and box size. To set this box setting, click the circuit on the tool bar and select box.

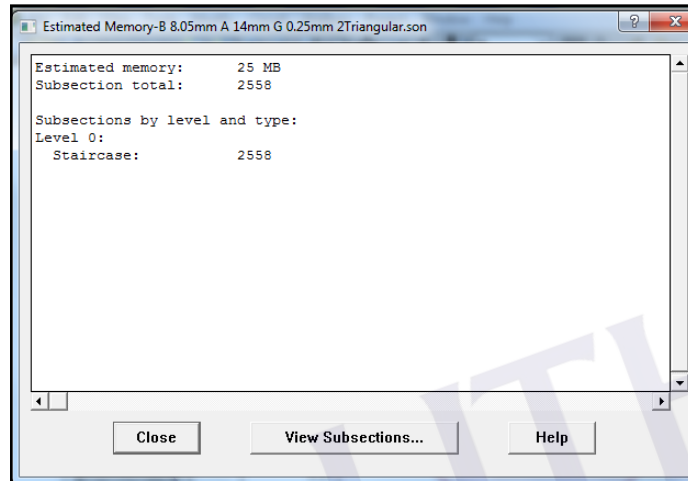


Figure 3.7: Estimated memory dialog box.

The estimated memory is important to display the value of size memory. This software only supports project design until 32MB memory size. To display the estimated memory box, click the circuit on the tool bar and select box. At the box setting, click the estimate memory button.

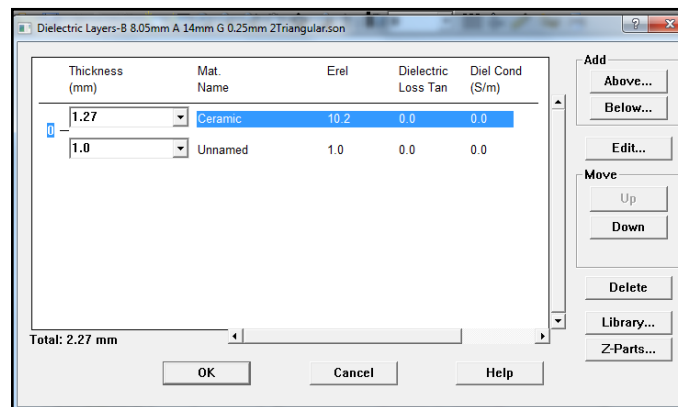


Figure 3.8: Dielectric layer dialog box.

The *Dielectric Layers dialog box* allows specification of the dielectric layers in the box including adding or deleting dielectric layers. A new geometry project always has two default layers whose material is *Air*, although the name “*Unnamed*” is displayed. The Project Editor level number appears on the left providing designer with an approximate side view of the circuit. A level is defined as the intersection of any two layers and is where the circuit metal is placed. This dielectric layer is the air above the actual microstrip. The layer thickness has absolutely no impact on execution time or accuracy. In this project, the material name for the dielectric layer is *Ceramic* with thickness 1.27mm and dielectric constant is 10.2 is set. To set this Metal Types, click the circuit on the tool bar and select *Dielectric Layer*.

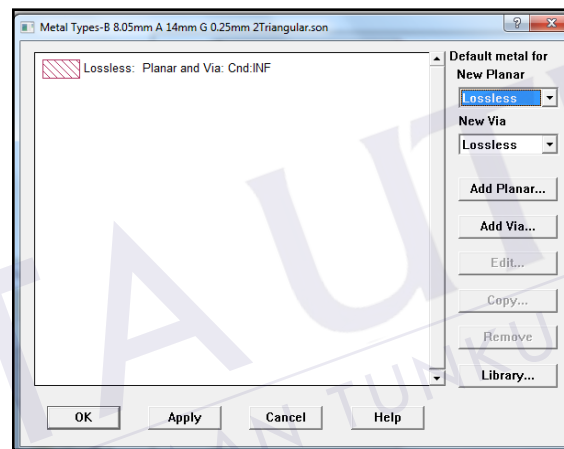


Figure 3.9: Metal type dialog box.

The *Metal Types* dialog box allows designer to define the characteristics of both *planar* and *via* metals for use in the circuit. A list of presently defined metals for your project appears in this dialog box. All geometry projects initially contain the metal type, *Lossless*, whose bulk conductivity is infinite (*INF*). In this project, the metal type *lossless: Planar and via: Cnd:INF* is set. To set this unit, click the circuit on the tool bar and select metal types.

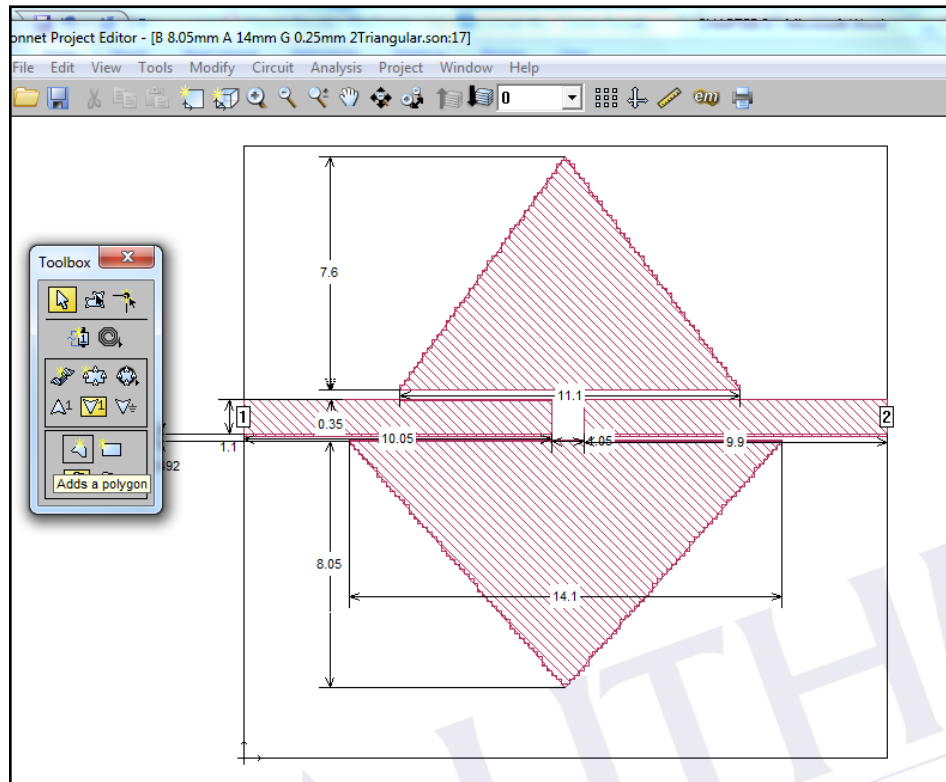


Figure 3.10: Sonnet project editor dialog box.

After all parameter have been set, the triangular patch resonator is drawn in the main window. The tool box is used to access the tools which enable designer to add or change objects in a circuit. *Port 1* and *port 2* were set in the project design. *Port 1* is set as input port and *port 2* as output port. To set port, click the tools on the tool bar and select add port. Dimension can set to the project to help measure dimensions of the circuit or to have dimensions shown in order to make the drawing clearer. To set dimension, click the tools on the tool bar and select add dimension.

REFERENCES

1. H.Iwasaki, A circularly polarized small-size microstrip antenna with a cross slot, *IEEE Trans Antennas propaget.*, vol.44, pp.1521-1528, Nov. 1996
2. R.R.Mansour, On the power handling capability of high temperature superconductive filters, *IEEE Trans, Microwave Theory Tech.*, vol.44, pp.1322-1338, July 1996
3. Z.Y.Shen, High-power HTS planar filters with novel back-side coupling, *IEEE Trans, Microwave Theory Tech*, vol.44, pp.984-986, June. 1996.
4. K. F. Raihn and G. L. Hey-Shipton, Folded dual-mode HTS microstrip band pass filter, *IEEE MTT-S Int. Microwave Symp. Dig.*, 2002, pp.1959–1962.
5. I. Wolff, Microstrip bandpass filter using degenerate modes of a microstrip ring resonator, *Electron. Lett.*, vol. 8, no. 12, pp. 302–303, June 1972.
6. J.-S. Hong and M. J. Lancaster, Microstrip bandpass filter using degenerate modes of a novel meander loop resonator, *IEEE Microwave Guided Wave Lett.*, vol. 5, pp. 371–372, Nov. 1995.
7. J. A. Curitis and S. J. Fiedziuszko, Miniature dual mode microstrip filters, *IEEE MTT-S Int. Microwave Symp. Dig.*, 1991, pp. 443–446.
8. R. R. Mansour, Design of superconductive multiplexers using single-mode and dual-mode filters, *IEEE Trans. Microwave Theory Tech.*, vol. 42, pp. 1411–1418, July 1994.
9. J.-S. Hong and M. J. Lancaster, Microstrip triangular patch resonators filters, *IEEE MTT-S Int. Microwave Symp. Dig.*, 2000, pp. 331–334
10. M. Cuhaci and D. S. James, Radiation from triangular and circular resonators in microstrip,” *IEEE MTT-S Int. Microwave Symp. Dig.*, 1977, pp. 438–441.

11. J. Helszajn and D. S. James, Planar triangular resonators with magnetic walls, *IEEE Trans. Microwave Theory Tech.*, vol. MTT-26, pp. 95–100, Feb. 1978
12. J. Helszajn, *Microwave Planar Passive Circuits and Filters*. New York: Wiley, 1994.
13. J.S. Hong and M. J. Lancaster, *Microstrip Filters for RF/Microwave Applications*. New York: Wiley, 2001.
14. J.S. Hong and S.Li, *Theory and Experiment of dual mode microstrip triangular patch resonators and filters*, *IEEE Trans. Microw. Theory Tech*, vol. 52, no. 4, pp. 1237-1243, Apr. 2004.
15. C. Lugo and J. Papapolymero, *Bandpass filter design using a microstrip triangular loop resonator with dual mode operation*, *IEEE Microw. Wireless Compon. Lett*, vol 15, no.7 pp. 75-477, Jul. 2005.
16. David M. Pozar. *Microwave Engineering*, Second Edition. John Wiley & Sons, Inc. pp.442; 1998.
17. David M. Pozar. *Microwave Engineering*, Second Edition. John Wiley & Sons, Inc. pp.160-162; 1998
18. Wen Hua Tu and kai Chang. Compact *Microstrip Bandstop Filter Using Open Stub and Spurline*. *IEEE Microwave and Wireless Components Letters*, vol.15, No.4, pp.268-270; April 2005.
19. Fred Gardiol. *Microstrip Circuits*. John Wiley & Sons, Inc. pp.51;1994
20. Wolf. *Microstrip Bandpass Filter Using degenerate Modes of a Microstrip Ring Resonator*, "Electronic Lett. Vol.8, No.12, 302
21. Chang, C.-Y. and C.-C Chen, *A novel coupling structure suitable for cross-coupled filters with folded quarter-wave resonators*, "IEEE Microw. Wirel. Compon. Lett., Vol. 13, No. 12, 517{519,2003.
22. Matsuo, M., H. Yabuki, and M. Makimoto, *Dual-mode stepped impedance ring resonator for bandpass fillter applications*," *IEEE Trans. Microw. Theory Tech.*, Vol. 49, No. 7, 1235 {1240, 2001.